Biochemical Pharmacology 83 (2012) 962–968

Contents lists available at SciVerse ScienceDirect

Biochemical Pharmacology

journal homepage: www.elsevier.com/locate/biochempharm

pH dependence on functional activity of human and mouse flavin-containing monooxygenase 5

Meike S. Motika, Jun Zhang, Erik C. Ralph, Mary A. Dwyer, John R. Cashman *

Human BioMolecular Research Institute, 5310 Eastgate Mall, San Diego, CA 92121, USA

ARTICLE INFO

Article history:
Received 8 October 2011
Accepted 5 January 2012
Available online 13 January 2012

Keywords:
Human and mouse flavin-containing monooxygenase 5
pH-dependent enzyme activity
hFMO5 D227K
hFMO5 Y228H

ABSTRACT

Flavin-containing monooxygenase (FMO) 5 belongs to a family of enzymes that catalyze the oxygenation of nucleophilic *N*- and *S*-containing compounds. The FMO enzyme family consists of five forms (FMOs1–5) that share about 50–60% sequence identity to each other. A comparison of FMOs showed that the pH-dependence profile for functional activity of FMO5 differed significantly from that of other FMO enzymes. The objective of this study was to examine the pH-dependence of FMO5 to gain insight into the mechanism of action of FMO5. Recombinant mouse and human FMO5 (mFMO5 and hFMO5, respectively) were expressed as maltose-binding fusion proteins from *Escherichia coli*, purified with affinity chromatography, and examined for their *N*-oxygenation functional activity at different pH values. hFMO5 showed a broader range and greater functional activity from pH 6 to 11 compared to mFMO5. mFMO5 lost almost all functional activity at pH 6, while hFMO5 maintained almost normal enzyme activity. In order to identify the amino acid residues involved in the effects of pH on hFMO5 and mFMO5 functional enzyme activity, pH-studies in the range of pH 6–9 were done with chimeras of recombinant mouse and human FMO5 and variants of both. Results of these studies and molecular modeling showed that residues responsible for the differences in the pH profile between mFMO5 and hFMO5 were located at positions 227 and 228 of the enzyme. Further variants were made to investigate the role of these amino acids. The results of this study may help to explain the mechanism of FMO function.

1. Introduction

Flavin-containing monooxygenase 5 (FMO5) belongs to a family of enzymes that catalyze the oxygenation of nucleophilic *N*- and *S*-containing compounds in an NADPH-dependent manner [1]. The enzyme family consists of five isozymes (FMO1–5) and 6 pseudogenes. The five FMO forms share about 50–60% sequence identity to each other and their expression is species- and tissue-dependent [2,3]. Hepatic expression of FMO5 is gender-independent in mice, rats and humans [4] whereas FMO3 is expressed in a gender-dependent way in mice and rats [3,5]. In contrast to *FMOs1–4*, that are all located on chromosome 1 in a 220 kb cluster, *FMO5* is located outside this cluster [2,6]. Also, FMO5 has a distinctive substrate specificity and although FMO5 represents ≥50% of the total FMO transcripts in both human [7] and mouse [5] liver, the contribution of FMO5 enzyme functional activity has not been clearly established. This is primarily due to a paucity of selective substrates. With typical FMO substrates such as methimazole or trimethylamine FMO5 does not show any functional activity [8], whereas it oxygenates long-chain phenothiazene analogs (i.e., 10-(*N,N*-dimethylaminooctyl)2-(trifluoromethyl)phenothiazene (8-DPT)) [8], *n*-octylamine [9,10], and *S*-methyl-esonarimod and its methoxy-analog [8,11].

A unique feature of mouse FMO5 (mFMO) is that when compared to the pH dependence of three other functional mFMOs (i.e., mFMO1, mFMO3, and mFMO4) and human FMO5 (hFMO5), it was found that the pH profile of mFMO5 differed significantly from that of all other FMO forms examined in the study [8]. The pH optima of mFMO1 and 3 displayed typical bell shape curves with a maximum around pH 8–10, whereas for human FMO5, 8-DPT *N*-oxygenation activity continued to increase from pH 7 to 11 [8]. There are many possible reasons for the different pH profile observed for mFMO5. For example, the slower overall turnover rate could possibly indicate a different rate-limiting step in the catalytic cycle of mFMO5. To date, the catalytic steps of pig FMO1 are known in some detail [12–16] and presumably, the other FMO isoforms follow a similar mechanism, but this might not be the case for all FMO forms. Also, it is possible that different ionizable amino acid residue(s) could be involved for mFMO1 and mFMO3 that are not involved with mFMO5. Thus, one possibility is that the

* Corresponding author. Tel.: +1 858 458 9305; fax: +1 858 458 9311.
E-mail address: jcashman@hbri.org (J.R. Cashman).

0006-2952/$ – see front matter © 2012 Elsevier Inc. All rights reserved.
doi:10.1016/j.bcp.2012.01.006

catalytic mechanism of FMO5 is distinct from that of other FMO enzymes.

In addition to the difference between the pH profiles of FMO5 and the other FMO forms, hFMO5 showed an even broader range of activity from pH 6 to 11 in comparison to mFMO5. Data obtained from pH studies of recombinant mouse and human FMO5 showed that mFMO5 lost almost all functional activity at pH 6, while hFMO5 maintains almost complete functional activity. This leads to the conclusion that in contrast to hFMO5, mFMO5 is less stable or less functionally active under slightly acidic conditions.

The objective of this study was to determine the pH dependence of mFMO5 and hFMO5 to gain insight into the mechanism of action of FMO5 enzymes. In order to locate the region, and/or amino acid residues involved in or responsible for the effects of pH on the human and mouse FMO5 enzymes, two sets of chimeras of mFMO5 and hFMO5 were designed, expressed, and purified and their functional activities at different pH values were compared. Finally, specific amino acids were changed by site-directed mutagenesis in both mFMO5 and hFMO5 to further examine the pK_a differences between both enzymes. Results of this study showed that the residues responsible for the pH profile distinction between mFMO5 and hFMO5 were located at positions 227 and 228 of the enzyme. Further mutants were made to investigate the role of the amino acids at these positions. Combined with other modeling, functional and kinetic studies described herein, these results may provide insight into the mechanism of FMO5 and reveal important interactions between substrate or cofactors of FMO and specific amino acid residues of the enzyme. In addition, the results may be relevant to other FMO enzymes if similar catalytic mechanisms and structural motifs are shared among different FMOs.

2. Materials and methods

2.1. Reagents

All chemicals and reagents were purchased from Sigma–Aldrich Chemical Co. (St. Louis, MO) in the highest purity commercially available. The components of the NADPH-generating system were purchased from Aldrich. Buffers and other reagents were purchased from VWR Scientific, Inc. (San Diego, CA). 10-(*N*,*N*-Dimethylaminooctyl)2-(trifluoromethyl)phenothiazine (8-DPT) and 8-DPT *N*-oxide were synthesized as previously described [8,17,18]. Plasmids pMal-hFMO5 [19] (Reddy 2009) and pMal mFMO5 [8] were prepared as previously described. The restriction endonucleases were purchased from New England Biolabs (Ipswich, MA).

2.2. Chimera-design of hm159, mh159, hm435, and mh435

Chimeric FMO5 hm159, mh159, hm435, and mh435 expression plasmids were created by swapping homologous restriction fragments of pMal-hFMO5 and pMal-mFMO5 plasmid DNAs. HindIII cuts both pMal-hFMO5 and pMal-mFMO5 plasmids between codon 159 and codon 160. NcoI cuts plasmids for both enzymes between codons 435 and 436.

pMal-*hFMO5* and pMal-*mFMO5* plasmids were digested with *Hind*III and *Nco*I. The vectors (i.e., pMal-*hFMO5 Hind*III, pMal-*mFMO5 Hind*III, pMal-hFMO5 *Nco*I, and pMal-mFMO5 *Nco*I) were then treated with Calf Intestinal Phosphatase (CIP) and DNA was purified and concentrated. pMal-*hFMO5* and pMal-*mFMO5* DNA inserts were ligated into either the *Hind*III or *Nco*I sites of the vectors in order to produce plasmids containing chimeric *FMO5* DNA. Finally, ligation products were transformed into MAX Efficiency DH5α competent *Escherichia coli* cells (Life Sciences Corporation, Carlsbad, CA). Plasmids purified from single colonies of each construct were sequenced to verify that the constructs possessed the correct sequence.

2.3. Chimera-design of hm229, mh229, hm370, and mh370

Due to the lack of convenient homologous restriction sites, the second set of chimeras were constructed by swapping homologous regions of pMal-*hFMO5* and pMal-*mFMO5* plasmid DNA through PCR amplification using chimera primers listed in Supplementary Material. The first swapping point was located between codons 229 and 230 of FMO5. The other was between codons 370 and 371. Chimeras were constructed in two steps of PCR reactions utilizing the FastStart High Fidelity PCR System (Roche Diagnostics, Indianapolis, IN): in a first PCR step, four human and four mouse FMO5 regions were amplified separately, each with 24 extended bases of mFMO5 and hFMO5, respectively, at one end. PCR reactions were run following the manufacturer's instructions.

In a second PCR reaction, human and mouse regions were annealed with their counterparts for eight PCR cycles and amplified for an additional 30 cycles after addition of the corresponding end primers (i.e., hF5fXbaI and mF5rPstIn for hm229 and hm370 FMO5, and mF5fXbaIn and hF5rPstI for mh229 and mh370 FMO5). The chimera PCR fragments were cloned into the expression vector restriction sites XbaI and PstI. All final plasmids were purified from single colonies of each construct and sequenced.

2.4. Site-directed mutagenesis of human and mouse FMO5 variants

Site-directed mutagenesis was done using a QuikChange Site-Directed Mutagenesis Kit (Stratagene, La Jolla, CA) following the manufacturer's instructions. Primers designed for site-directed mutagenesis of mFMO5 and hFMO5 were listed in Supplementary Material. The final plasmids purified from single colonies of each construct were sequenced to verify the presence of the intended mutations and absence of additional mutations.

2.5. Expression and purification of human–mouse MBP-FMO5 chimera and human or mouse MBP-FMO5 and variants

Expression vectors for the eight FMO5 chimeras and mFMO5 and hFMO5 variants were cloned into pMal-2c (New England Biolabs) with site-directed mutagenesis methods as described previously [20,21]. Briefly, the FMO5 enzymes were expressed as *N*-terminal maltose-binding fusion proteins (i.e., MBP-FMO5). After transformation of pMal-MBP-*FMO5* plasmid into *E. coli* DH 1α cells, cells were grown at 37 °C in SOC medium containing 100 μg/ml ampicillin to an absorbance of 0.4–0.5 at 600 nm. IPTG (0.2 mM) and riboflavin (0.05 mM) was added, and the cells were further incubated overnight at room temperature and finally harvested by centrifugation at 6000 × *g* for 10 min.

The following procedures including the purification process were carried out at 4 °C. The cell pellet was resuspended in lysis buffer as described previously [22]. The cell suspension was stirred on ice for 30 min, and the cells were disrupted by sonication, centrifuged and the solubilized FMO5 protein in the resulting supernatant was purified as previously described for FMO3 [23]. Bound MBP-FMO5 protein was then eluted with 3 mM maltose or a linear maltose gradient of 0–100% buffer B (buffer A with 10 mM maltose) over 100 min at 1 ml/min. Buffer A contained 50 mM potassium phosphate buffer, pH 8.5 and 15 μg/ml FAD. Eluted fractions (each 5 ml) containing the purified fusion protein were pooled and concentrated with a Centriprep centrifugal filter unit with Ultracel-30 membrane or an Amicon Ultra-15 centrifugal filter unit with an Ultracel-50 filter (Millipore, Billerica, MA).

2.6. Determination of protein concentrations of MBP-FMO5 chimera

The concentration of purified MBP-FMO5 chimeras as well as hFMO5 or mFMO5 and their variants was determined by SDS-PAGE and Coomassie blue staining and compared with a bovine serum albumin (BSA) standard as described previously [23].

2.7. Enzyme assays

2.7.1. N-Oxygenation of 8-DPT by FMO5

The *N*-oxygenation of 8-DPT was determined by HPLC analysis as previously described [21–23]. A standard incubation mixture contained 100 mM potassium phosphate buffer at different pH values (i.e., pH 6.0, 6.3, 6.7, 7.0, 7.3, 7.7, and 8.0), 0.4 mM $NADP^+$, 0.4 mM glucose-6-phosphate, 4 IU glucose-6-phosphate dehydrogenase, 0.25 mM diethyleneaminepentacetic acid (DETAPAC), and 80 μg MBP-FMO5. Incubations were initiated by the addition of substrate to a final concentration of 200 μM. After incubation for 20 min with constant shaking under aerobic conditions at 37 °C the incubation was stopped by addition of cold dichloromethane. Metabolites and remaining substrate were isolated by extraction, evaporated and the residue was analyzed with a Hitachi HPLC system (Hitachi L-7200 autosampler and L-7100 pump interfaced to a Hitachi L-7400 UV detector, Hitachi, San Jose, CA). Chromatographic separation of analytes was done on an Axxi-Chrom's normal phase analytical column (250 mm × 4.6 mm 5 μm, silica) with a mobile phase of 80% MeOH/20% Isopropanol/0.025% $HClO_4$. The flow rate was 1.6 ml/min and the total run time was 8.5 min. The wavelength for UV detection was set at 243 nm. The retention times for 8-DPT and 8-DPT *N*-oxide were 5.8, and 4.1 min, respectively.

2.7.2. Optimization of FMO enzyme assays

The assay conditions for FMO-mediated *N*-oxygenation functional activity has previously been described and successfully used for various studies [21] and thus were adapted with only minor changes for the pH study described herein. The *N*-oxygenation of 8-DPT HCl was determined by HPLC analysis as described above with incubation mixtures containing a buffer mix consisting of 0.1 M ACES, 52 mM Tris, and 52 mM ethanolamine at different pHs (i.e., pH 6.0, 6.3, 6.7, 7.0, 7.3, 7.7, 8.0, and 9.0), 0.4 mM $NADP^+$, 0.4 mM glucose-6-phosphate, 4 IU glucose-6-phosphate dehydrogenase, 0.25 mM DETAPAC, and 40 μg MBP-FMO5. The advantage of this buffer system over phosphate buffer that was used previously is that: (a) its ionic strength was virtually constant over a wide range of pH values, (b) its buffer capacity was much better than that of phosphate buffer over the pH range tested and (c) the pH did not change upon dilution [24]. Incubations were initiated by the addition of substrate to a final concentration of 400 μM. After a 20-min incubation the samples were processed and analyzed via HPLC as described above.

2.8. FMO5 structure prediction

A model of the hFMO5 (accession number: AAH35687) three-dimensional structure was determined using the iterative threading assembly refinement (I-tasser) algorithm [25–27]. Using Pymol [28], the hFMO5 structural model with the highest confidence score (C = 0.05) was then aligned with the three dimensional structures for NADH peroxidase from *Streptococcus faecalis* (PDB Code: 1NPX) and glutathione reductase from *E. coli* (PDB Code: 1GET), two proteins previously used in FMO molecular models [29].

2.9. Data analysis

Incubations were done in duplicate or triplicate and for data analysis a nonlinear regression curve fit tool using a Michaelis-Menten model in Graphpad software (Graphpad Prism, Version 3.00, San Diego, CA) was utilized. Data obtained was presented as the mean of the best fit value ± standard error. Statistical analysis was also done using Graphpad Prism software (Version 3). A one-way ANOVA test followed by a Kruskal–Wallis post test were used to judge statistical significance at $p < 0.05$. Statistical significance was judged at $p < 0.05$.

3. Results

3.1. FMO5 expression and purification

Human and mouse FMO5 as well as their variants were expressed as MBP-fusion proteins in *E. coli*. With the exception of the hm229 chimera, all proteins were obtained in yields between 40 and 200 mg for 6 L bacterial cultures with comparable purity and 8-DPT *N*-oxygenation specific activity.

Results from the determination of kinetic parameters (i.e., V_{max} and K_m) for FMO5-mediated 8-DPT HCl *N*-oxygenation showed that a greater substrate concentration was more useful for routine analysis (K_m = 117 μM and V_{max} = 3.2 nmol/min/mg FMO5) (Fig. 1A and B). The K_m was not expected to be different at different pH values and thus, a substrate concentration of 400 μM was a useful saturating concentration used for evaluating pH values examined between 6 and 8 (Fig. 1). Therefore, in the pH-

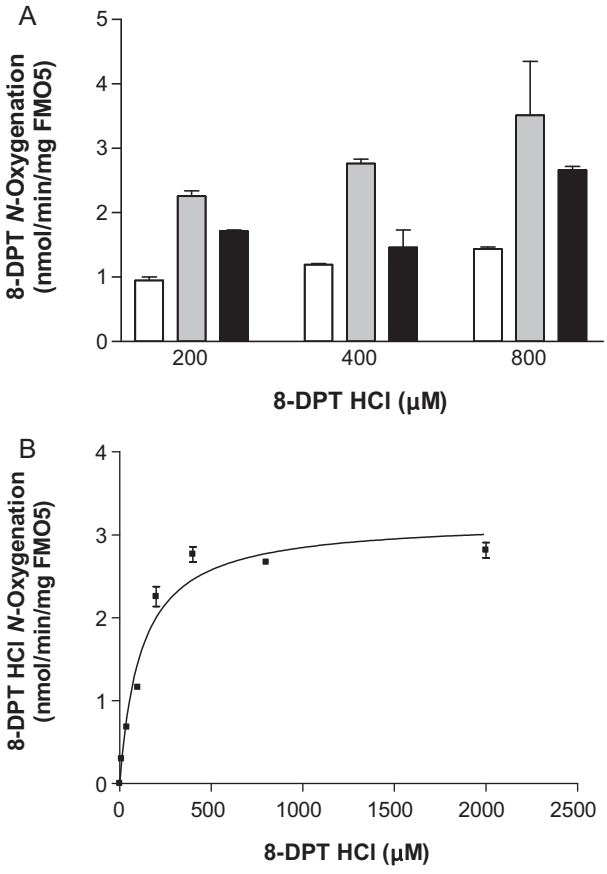

Fig. 1. Kinetics of 8-DPT *N*-oxygenation as a function of pH and substrate concentration. (A) Comparison of mFMO5-mediated 8-DPT HCl *N*-oxygenation at different pH values and substrate concentrations. Studies done at pH 6 was shown as white bars, pH 8.4 as gray bars, and pH 11 as black bars. Values are the mean ± SEM. No significant differences ($p > 0.05$; ANOVA and Kruskal–Wallis post test) were observed between values measured at the same pH with the exception of pH 6 at 200 and 800 μM ($p = 0.02$) and pH 11 at 400 and 800 μM ($p = 0.01$) 8-DPT. (B) Determination of kinetic parameters for 8-DPT HCl *N*-oxygenation with mFMO5 at pH 8.4. Values are the mean ± std. error ($n = 3$).

profile experiments of mFMO5 and hFMO5 variants, a final 8-DPT HCl concentration of 400 μM was used. The pH profiles of mFMO5 and hFMO5 were obtained with a number of substrate concentrations and the results showed no significant differences (i.e., p values >0.17) with the exception of pH 6 at 200 and 800 μM ($p = 0.02$) and pH 11 at 400 and 800 μM ($p = 0.01$) 8-DPT (Fig. 1).

3.2. pH-dependence of human and mouse FMO5

The pH-dependence for hFMO5 and mFMO5 was studied and pK_a values were determined in the range of pH 6–8. As shown previously, the pK_a of mFMO5 (i.e., 7.2 ± 0.1) was significantly greater than that of hFMO5 (i.e., 6.6 ± 0.1) [8].

3.3. pH-dependence of hm159, mh159, hm435, and mh435 chimeras

The pH-dependent 8-DPT *N*-oxygenation by MBP-FMO5 chimeras hm159, mh159, hm435, and mh435 was analyzed and pH profiles were evaluated with regards to a decrease in functional activity at low pH values. A comparison of hm159 and mh159, showed that amino acid residues 1–159 of hFMO5 were not involved in the increased stability observed at lower pH for hFMO5 because the pH profile of mh159 was close to that of hFMO5 whereas the decrease in functional activity of hm159 was steeper at low pH that resembled the pH profile of mFMO5. A comparison of the other two chimeras (i.e., hm435 and mh435) showed a difference in functional activity (i.e., a decrease at pH 6 was not as pronounced). Nevertheless, the pH profile for hm435 appeared similar to that of hm159 (e.g., pH 7.0 and 7.3) and similar to that of wild-type mFMO5, whereas the pH profile of mh435 appeared to follow the profile of mh159 (e.g., 7.0–8.0) (Fig. 2). The conclusion from these chimera studies was that the amino acid(s) most likely responsible for the functional activity of hFMO5 at lower pH was located between amino acid residues 160 and 434.

3.4. pH-dependence of hm229, mh229, hm370, and mh370

Based on data from the first set of experiments with hm and mh FMO5 chimeras described above (i.e., hm159, mh159, hm435, and mh435 chimeras), the region of interest where the amino acid residue(s) involved in greater functional activity of hFMO5 (below pH 7) was narrowed down to amino acid residues 160–434. A set of four new chimeric FMO5 enzymes representing one part hFMO5 and one part mFMO5 were designed, expressed and purified in order to determine their pH profiles and localize the amino acid(s) of interest. The pH profile of hm229 FMO5 could not be determined due to very poor levels of expression. The pH profiles for FMO5

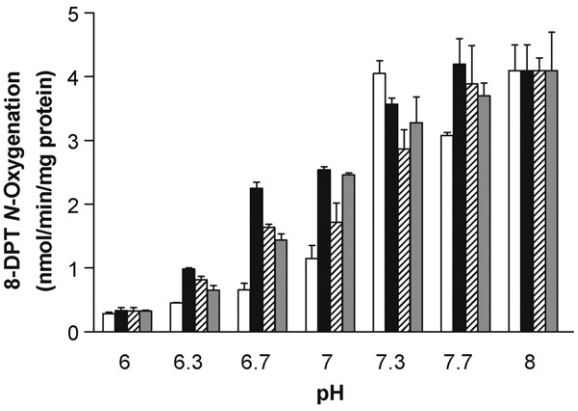

Fig. 2. Mouse/human chimera and their pK_a values derived from 8-DPT *N*-oxygenation assays at pH 6–8. hm159, white bars; mh159, black bars; hm435 hatched bars, mh435, gray bars. Values are the mean ± std. error ($n = 3$).

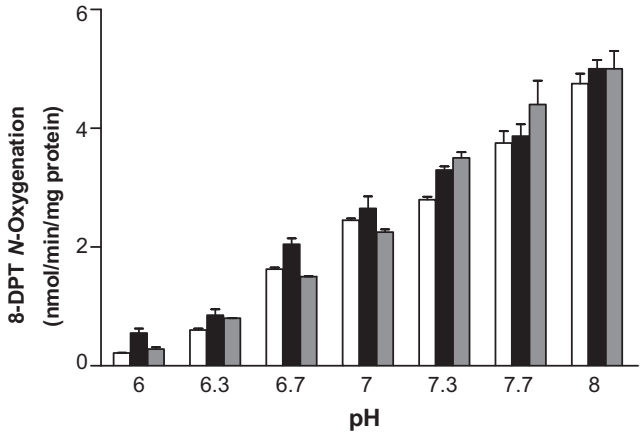

Fig. 3. Mouse/human chimera and their pK_a values derived from 8-DPT *N*-oxygenation at pH 6–8. mh 229 white bars; hm370, black bars; mh370, hatched bars. Values are the mean ± std. error ($n = 3$).

functional activity for the other three chimeras analyzed were determined and shown in Fig. 3.

3.5. Summary: pH-dependence of human and mouse FMO5 chimera

Chimeras of hFMO5 and mFMO5 with swapping points at amino acids 229, 370, and 435 did not differ significantly in their pH-dependent functional activity profiles (Figs. 2 and 3). Thus, amino acid residue(s) involved in the greater functional activity of hFMO5 below pH 7 were most likely located between amino acids 160 and 229 because only chimeras after codon 159 showed significant differences.

Sequence alignment of mFMO5 and hFMO5 showed that within this specific region, six amino acids of hFMO5 differed from mFMO5. Utilizing site-directed mutagenesis, these amino acids were changed in hFMO5 to the ones found in mFMO5. The hFMO5 variants were expressed and purified and their pH profile was determined between pH 6 and 9 using *N*-oxygenation of 8-DPT HCl as an indication of functional activity.

3.6. pH-dependence of human and mouse FMO5 variants

The pH profile of mFMO5 as well as hFMO5 and hFMO5 cDNA-expressed variants that were purified was determined after optimization of assay conditions. The results of wild-type hFMO5 and mFMO5 are shown in Fig. 4. The studies were done in a similar

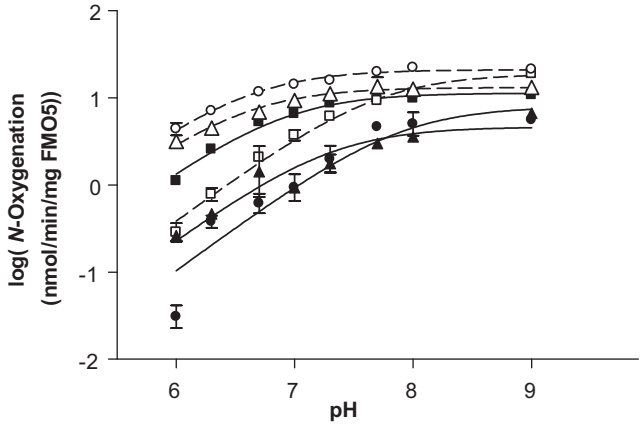

Fig. 4. pK_a determination of wild-type human and mouse FMO5 and of human and mouse FMO5 variants using 8-DPT *N*-oxygenation. ■ hFMO5; □ mFMO5; ▲ hFMO5 D227K; Δ mFMO5 K227D; ● hFMO5 Y228H; ○ mFMO5 H228Y. Values are the mean ± std. error ($n = 3$).

Table 1
pK_a values for *N*-oxygenation of 8-DPT by wild type and human and mouse FMO5.

Variant	pK_a[a]
Wild-type hFMO5	6.9 ± 0.1
Wild-type mFMO5	7.7 ± 0.1
hFMO5 Q170K	6.6 ± 0.1
hFMO5 G182E	6.6 ± 0.1
hFMO5 Q206H	6.5 ± 0.0
hFMO5 D227K	7.3 ± 0.1
hFMO5 Y228H	7.9 ± 0.2

[a] Data is presented as the mean of the best fit value ± std. error (n = 3).

fashion to those obtained with the original assay conditions that provided a pK_a of 7.7 ± 0.1 for mFMO5 and a pK_a of 6.9 ± 0.1 for hFMO5 [8]. The pK_a values determined for wild-type mFMO5 and hFMO5 as well as hFMO5 variants are summarized in Table 1.

The data clearly showed that replacement of tyrosine at position 228 with histidine increased the pK_a of hFMO5 to the level of wild-type mFMO5, whereas the other hFMO5 mutations did not have a significant influence on the pK_a of hFMO5.

To confirm this result, the mouse counterpart with the amino acid of the corresponding human enzyme were made and as suspected, mFMO5 H228Y had a decreased pK_a value comparable to the wild-type mouse enzyme (Table 2). In addition, the mouse counterpart to hFMO5 D227K (i.e., mFMO5 K227D) was made and tested because its pK_a also was increased compared to wild-type hFMO5, even though this increase was lower than that of hFMO5 Y228H (Fig. 4 and Table 1). Also, several variants of hFMO5 Y228 were made in order to evaluate the effect of different amino acids at this position. The results are also summarized in Table 2.

As shown herein, the mouse enzyme that contained a tyrosine at position 228 instead of a histidine (mFMO5 H228Y) had a significantly decreased pK_a value compared to the wild-type enzyme. The same observation was made for the K227D variant of mFMO5. Changing the amino acid tyrosine in wild-type hFMO5 to three of the amino acids examined (i.e., lysine, alanine, and arginine) also significantly increased the pK_a value of human FMO5. However, changing tyrosine to phenylalanine did not make a significant difference in the pK_a value (pK_a of 6.9 and 6.7 for wild-type hFMO5 and hFMO5 Y228F, respectively). Overall, the low pK_a value appeared to be due to the amino acids at position 227 and 228 in the human enzyme and thus they are at least in part responsible for the increased enzyme functional activity at low pH.

Table 2
pK_a values for 8-DPT *N*-oxygenation by wild-type mouse and wild-type human FMO5 and hFMO5 Y228 variants.

Variant	pK_a[a]
Wild-type hFMO5	6.9 ± 0.1
Wild-type mFMO5	7.7 ± 0.1
hFMO5 D227K	7.3 ± 0.1
mFMO5 K227D	6.6 ± 0.0
hFMO5 Y228H	7.9 ± 0.2
mFMO5 H228Y	6.6 ± 0.0
hFMO5 Y228K	8.0 ± 0.1
hFMO5 Y228A	7.8 ± 0.1
hFMO5 Y228F	6.7 ± 0.0
hFMO5 Y228R	7.7 ± 0.1

[a] Data is presented as mean of the best fit value ± std. error (n = 3).

3.7. FMO5 structure prediction

hFMO5 structure modeling and enzyme kinetic data suggested that the largest enzymatic functional activity may be modulated by changes in hydrogen bonding and/or the electrostatic potential in the substrate or cofactor binding domain. Specifically, mutation of hFMO5 tyrosine 228 to histidine may alter hydrogen bonding of this residue to the $NADP^+$ cofactor (Fig. 5). Moreover, mutation of hFMO5 residue 228 to lysine, arginine, or histidine afforded kinetic parameters similar to that of mFMO5. In contrast, mutation of hFMO5 residue 228 to phenylalanine had little effect. Mutation of the mFMO5 residue 228 histidine to tyrosine resulted in optimal functional enzyme activity and a pK_a similar to hFMO5. Consistent with this hypothesis, a charge reversal at position 227 in either human or mouse switches the pH dependence of the functional enzyme activity.

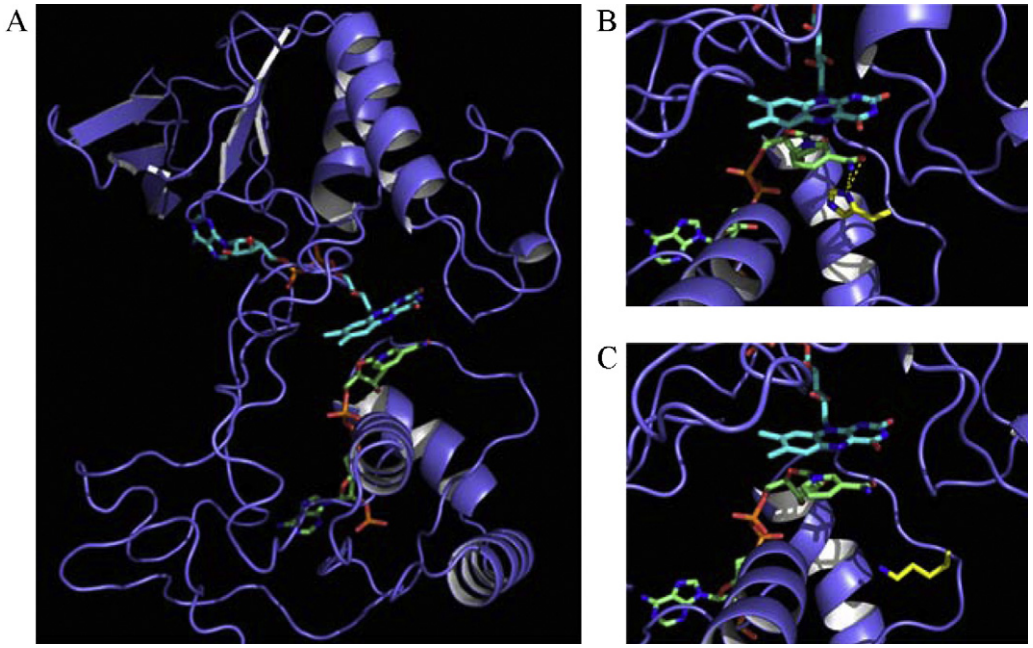

Fig. 5. hFMO5 structural models. (A) hFMO5 full-length structure modeled with FAD (cyan) and $NADP^+$ (green) cofactors through alignment with NADH peroxidase (1NPX) and glutathione reductase (1GET) for FAD and NADP placement, respectively [29]. (B) Structural model of the hFMO5 Y228H (yellow) mutation with putative hydrogen bonds to FAD amide highlighted. (C) Structural model of the hFMO5 D227K (yellow) mutation.

4. Discussion

Compared with mFMO5 it was observed that hFMO5 possessed a significantly different pH profile based on evaluation of a selective functional substrate for *N*-oxygenation. hFMO5 had a significantly lower pK_a compared to mFMO5. Using chimera studies involving both mouse and human enzymes the region of amino acids that were responsible for the pK_a shift of FMO5 was identified and alignment of mFMO5 and hFMO5 sequences showed that this was a highly conserved region that was only distinguishable by the presence of six different amino acids. Site-directed mutagenesis studies of the six amino acids were done and the pH profiles of the resulting variants were determined. The resulting data clearly showed that the residues responsible for the difference in the pH profile for mFMO5 and hFMO5 was associated with positions 227 and 228 of FMO5. While many factors could contribute to the pH profile for enzyme catalysis, it has been reported that pH-dependent activity of an enzyme is often determined by pK_a values of only one or a few key ionizable amino acids within the enzyme, primarily in the active-site cleft [30]. According to a human FMO3 homology structure model developed based on four related proteins [31], the FMO3 amino acids D226/N227 (i.e., equivalent to position 227 and 228 of FMO5) lie on the surface of the protein close to the entrance of a passage connecting the space between the two cofactor binding domains (i.e., NADPH and FAD). A new FMO5 model (Fig. 5) recapitulates this hypothesis previously developed for models of FMO1 and FMO3 [29]. It may be that position 227 of FMO5 constitutes a peripheral binding site for substrate or co-factors.

For amino acid residue 228 of FMO5, pi–pi stacking interactions or electrostatics may be important and influence the pK_a of the enzyme. In wild-type hFMO5, tyrosine 228 may make a hydrogen bond with $NADP^+$. If tyrosine 228 is replaced by a histidine, this interaction may be interrupted due to protonation at a lower pH. This would also be the case if tyrosine 228 was replaced by lysine or arginine. The data obtained supports this hypothesis, because a significantly increased pK_a for both hFMO5 Y228R and hFMO5 Y228K (i.e., 7.7 ± 0.1 and 8.0 ± 0.1, respectively) was observed compared to the pK_a for wild-type hFMO5 (i.e., 6.9 ± 0.1). Non-polar amino acids such as phenylalanine or alanine might not be able to interact because of lack of a polar or hydrogen-bonding group. Indeed, we observed a significantly increased pK_a value for hFMO5 Y228A (7.8 ± 0.1). However, for hFMO5 Y228F the pK_a value was closer to that of the wild-type enzyme (6.7 ± 0.0). Therefore, the contribution of amino acid 228 to the pK_a is apparently not a simple interaction.

Protein conformational changes may also have an influence on FMO5 pK_a behavior. Thus, the similar pK_a values observed for Y228 and F228 could be explained by steric similarity between the two amino acid side chains. It is possible that an aromatic ring is required in this position and that changing this might have an effect on neighboring residues such as D227. For example, in the case of a tyrosine at position 228 and an aspartic acid at position 227 it is possible that a hydrogen bond could form with $NADP^+$. Evidence for this comes from mutagenesis of an aspartic acid at position 227 to a lysine that resulted in an increased pK_a (i.e., 7.3 ± 0.1). Shifting this residue by changing the size of the amino acid at position 228 might also prevent this interaction and lead to an altered pK_a.

Amino acid residues may be sensitive to both electrostatic and structural changes of other amino acids that are located in the immediate vicinity. Thus, an amino acid change could have an effect on pK_a values in the case where neighboring residues exert a steric influence as described for the substitution of asparagine with aspartic acid at position 35 in *Bacillus circulans* xylanase [30]. The substitution of a neutral amino acid asparagine with an acidic aspartic acid (pK_a 3.7) in xylanase elevated the pK_a values of neighboring residues E78 and E172, likely due to charge repulsion. As a result, the pH optimum of xylanase was shifted from 5.7 to 4.6 [30]. In addition, protonation or deprotonation of amino acids may also help stabilize other proximal residues and amino acid substitution might lead to destabilization and an altered pH. For example, for polyketide synthase, stabilization and promotion of a thiolate anion at C164 by H303, as an imidazolium cation, was reported. Thus, upon substitution of H303, in addition to reactivity, the pK_a value of the C164 changed [32]. It is possible that for FMO5, amino acid changes at position 227 and 228 may not only influence the charge of the protein itself but also alter pK_a values of surrounding residues or stabilize/destabilize these depending on the charge of the amino acid in these positions. Thus, although current three-dimensional models suggest that D227 and Y228 lie close to the surface of the protein, they could have an impact on amino acids that are closer to the substrate binding site or that influence NADPH binding or $NADP^+$ release. A model of FMO5 (Fig. 5) shows that these amino acids are proximal to the FAD binding domain or close to the substrate binding domain.

The pI of the enzyme could also affect its pH-dependent activity profile. The theoretical pI of hFMO5 and mFMO5 are 6.3 and 7.2, respectively. It is possible that the enzyme has to be negatively charged to function properly. Because hFMO5 has a lower pI than mFMO5, it will tend to keep its negative charge longer at lower pH. Thus, hFMO5 has a negative charge above pH 6 whereas mFMO5 is negatively charged above pH 7 and thus its functional activity decreases faster in comparison to hFMO5 below this pH. This was observed in the pH-functional activity profiles shown in this study. A calculation of the pIs of certain variants' showed an increase for hFMO5 D227K to 6.5 and a decrease for mFMO5 K227D to 6.8 supporting the results of this study. FMO5 is negatively charged at its pH optimum. Assuming the enzyme functions best when it is negatively charged, a substitution of asparagine with aspartic acid and the resulting change of pI could lead to a differently charged enzyme at low pH. Alternatively, the pI of FMO5 could simply be a requirement for stabilization in the surrounding environment rather than affecting substrate binding or turnover by controlling the charge of the enzyme [30].

In conclusion, pH-dependent functional activity differences of hFMO5 and mFMO5 were compared and the amino acids responsible for the changes in pK_a values were identified. Changing aspartic acid at position 227 to lysine or changing tyrosine at position 228 to histidine increased the pK_a of hFMO5 from 6.9 to 7.3 and 7.9, respectively. Accordingly, an amino acid change of K227 to D227 or H228 to T228 lowered the pK_a from 7.7 in wild-type mFMO5 to 6.6 and 6.5, respectively. To address the question of how FMO5 pH-dependent functional activity is changed by these amino acids and whether the residues at position 227 and 228 interact with the cofactor directly or whether the affect neighboring residues will require further investigation.

Acknowledgments

This work was supported by funds from HBRI. The authors would like to thank Rob Reddy for contributing to FMO5 purification, Karl Okolotowicz for synthesis of 8-DPT and Professor Bernd Clement for helpful discussions. We also thank Professor Y. Zhang (University of Michigan) for help with the model of FMO5.

Appendix A. Supplementary data

Supplementary data associated with this article can be found, in the online version, at doi:10.1016/j.bcp.2012.01.006.

References

[1] Cashman JR, Zhang J. Human flavin-containing monooxygenases. Annu Rev Pharmacol Toxicol 2006;46:65–100.
[2] Phillips IR, Dolphin CT, Clair P, Hadley MR, Hutt AJ, McCombie RR, et al. The molecular biology of the flavin-containing monooxygenases of man. Chem Biol Interact 1995;96:17–32.
[3] Cashman JR. Structural and catalytic properties of the mammalian flavin-containing monooxygenase. Chem Res Toxicol 1995;8:166–81.
[4] Cherrington NJ, Cao Y, Cherrington JW, Rose RL, Hodgson E. Physiological factors affecting protein expression of flavin-containing monooxygenases 1, 3 and 5. Xenobiotica 1998;28:673–82.
[5] Janmohamed A, Hernandez D, Phillips IR, Shephard EA. Cell-, tissue-, sex- and developmental stage-specific expression of mouse flavin-containing monooxygenases (Fmos). Biochem Pharmacol 2004;68:73–83.
[6] Hernandez D, Janmohamed A, Chandan P, Phillips IR, Shephard EA. Organization and evolution of the flavin-containing monooxygenase genes of human and mouse: identification of novel gene and pseudogene clusters. Pharmacogenetics 2004;14:117–30.
[7] Zhang J, Cashman JR. Quantitative analysis of FMO gene mRNA levels in human tissues. Drug Metab Dispos 2006;34:19–26.
[8] Zhang J, Cerny MA, Lawson M, Mosadeghi R, Cashman JR. Functional activity of the mouse flavin-containing monooxygenase forms 1, 3, and 5. J Biochem Mol Toxicol 2007;21:206–15.
[9] Cherrington NJ, Falls JG, Rose RL, Clements KM, Philpot RM, Levi PE, et al. Molecular cloning, sequence, and expression of mouse flavin-containing monooxygenases 1 and 5 (FMO1 and FMO5). J Biochem Mol Toxicol 1998;12:205–12.
[10] Overby LH, Buckpitt AR, Lawton MP, Atta-Asafo-Adjei E, Schulze J, Philpot RM. Characterization of flavin-containing monooxygenase 5 (FMO5) cloned from human and guinea pig: evidence that the unique catalytic properties of FMO5 are not confined to the rabbit ortholog. Arch Biochem Biophys 1995;317:275–84.
[11] Ohmi N, Yoshida H, Endo H, Hasegawa M, Akimoto M, Higuchi S. S-oxidation of S-methyl-esonarimod by flavin-containing monooxygenases in human liver microsomes. Xenobiotica 2003;33:1221–31.
[12] Beaty NB, Ballou DP. The oxidative half-reaction of liver microsomal FAD-containing monooxygenase. J Biol Chem 1981;256:4619–25.
[13] Beaty NB, Ballou DP. The reductive half-reaction of liver microsomal FAD-containing monooxygenase. J Biol Chem 1981;256:4611–8.
[14] Poulsen LL, Ziegler DM. The liver microsomal FAD-containing monooxygenase. Spectral characterization and kinetic studies. J Biol Chem 1979;254:6449–55.
[15] Ziegler DM, Ansher SS, Nagata T, Kadlubar FF, Jakoby WB. N-methylation: potential mechanism for metabolic activation of carcinogenic primary arylamines. Proc Natl Acad Sci USA 1988;85:2514–7.
[16] Jones KC, Ballou DP. Reactions of the 4a-hydroperoxide of liver microsomal flavin-containing monooxygenase with nucleophilic and electrophilic substrates. J Biol Chem 1986;261:2553–9.
[17] Nagata T, Williams DE, Ziegler DM. Substrate specificities of rabbit lung and porcine liver flavin-containing monooxygenases: differences due to substrate size. Chem Res Toxicol 1990;3:372–6.
[18] Lomri N, Yang Z, Cashman JR. Expression in *Escherichia coli* of the flavin-containing monooxygenase D (form II) from adult human liver: determination of a distinct tertiary amine substrate specificity. Chem Res Toxicol 1993;6:425–9.
[19] Reddy RR, Ralph EC, Motika MS, Zhang J, Cashman JR. Characterization of human FMO3 and FMO5 expressed as maltose binding protein fusions. Drug Metab Dispos 2010;38:2239–45.
[20] Zhang J, Tran Q, Lattard V, Cashman JR. Deleterious mutations in the flavin-containing monooxygenase 3 (FMO3) gene causing trimethylaminuria. Pharmacogenetics 2003;13:495–500.
[21] Brunelle A, Bi YA, Lin J, Russell B, Luy L, Berkman C, et al. Characterization of two human flavin-containing monooxygenase (form 3) enzymes expressed in *Escherichia coli* as maltose binding protein fusions. Drug Metab Dispos 1997;25:1001–7.
[22] Lattard V, Zhang J, Tran Q, Furnes B, Schlenk D, Cashman JR. Two new polymorphisms of the FMO3 gene in Caucasian and African-American populations: comparative genetic and functional studies. Drug Metab Dispos 2003;31:854–60.
[23] Motika MS, Zhang J, Zheng X, Riedler K, Cashman JR. Novel variants of the human flavin-containing monooxygenase 3 (FMO3) gene associated with trimethylaminuria. Mol Genet Metab 2009;97:128–35.
[24] Ellis KJ, Morrison JF. Buffers of constant ionic strength for studying pH-dependent processes. Methods Enzymol 1982;87:405–26.
[25] Roy A, Kucukural A, Zhang Y. I-TASSER: a unified platform for automated protein structure and function prediction. Nat Protoc 2010;5:725–38.
[26] Zhang Y. I-TASSER server for protein 3D structure prediction. BMC Bioinformatics 2008;9:40.
[27] Roy A, Xu D, Jonathan P, Zhang Y. A protocol for computer-based protein structure and function prediction. J Visualized Exper 2011;57:e3259.
[28] The PyMOL Molecular Graphics System, Version 1.3, Schrödinger, LLC.
[29] Cashman JR. Flavin Monooxygenases. In: Ioannides C, editor. Enzyme systems that metabolize drugs and other xenobiotics, vol. 3. John Wiley & Sons, Ltd.; 2002. p. 67–93.
[30] Joshi MD, Sidhu G, Pot I, Brayer GD, Withers SG, McIntosh LP. Hydrogen bonding and catalysis: a novel explanation for how a single amino acid substitution can change the pH optimum of a glycosidase. J Mol Biol 2000;299:255–79.
[31] Borbas T, Zhang J, Cerny MA, Liko I, Cashman JR. Investigation of structure and function of a catalytically efficient variant of the human flavin-containing monooxygenase form 3. Drug Metab Dispos 2006;34:1995–2002.
[32] Jez JM, Noel JP. Mechanism of chalcone synthase. pKa of the catalytic cysteine and the role of the conserved histidine in a plant polyketide synthase. J Biol Chem 2000;275:39640–6.